



Application of Surfactant Modified Kono-Boue Clay Nanoparticles in Oil Recovery

Ogochukwu Vivian Udeh , Joshua Lelesi Konne* , Grace Agbizu Cooney ,
Godwin Chukwuma Jacob Nmegbu

1. Rivers State University, Rivers State, Nigeria. E-mail: ogoudeh24@gmail.com
2. Faculty of Science, Nigeria. E-mail: konne.joshua@ust.edu.ng
3. Faculty of Science, Nkpolu-Oroworukwo, Nigeria. E-mail: cookey.grace@ust.edu.ng
4. Department of Petroleum Engineering, Rivers State University, Port Harcourt, Nigeria. E-mail: nmegbu.godwin@ust.edu.ng

ARTICLE INFO	ABSTRACT
<p>Article History: Received: 16 October 2024 Revised: 03 December 2024 Accepted: 10 December 2024 Published: 12 January 2025</p> <p>Article type: Research</p> <p>Keywords: Enhanced Oil Recovery, Kono-Boue Clay, Micro Model, Nanoparticles, SDS- Mediated</p>	<p>Sodium Dodecyl Sulphate (SDS) mediated Kono-Bono (KB) clay nanoparticles (NPs) applied in Enhanced Oil Recovery (EOR) have been investigated for the first time. This was done using synthesized KB clay NPs as a control and SDS-treated KB clay NPs experiments in a micro model to determine the oil recovery rate. The samples were prepared by dissolving 15 g of KB clay in a mixture of 450 ml of de-ionized water and 150 ml of varying SDS concentrations, magnetically stirred, dried at 110 °C for 90 minutes, and further calcined at 900 °C in a muffle furnace for 120 minutes. The samples were characterized with Fourier Transform infrared (FT-IR) Spectroscopy, Scanning Electron Microscopy (SEM), X-ray fluorescence (XRF), and X-ray Diffraction (XRD), respectively. FT-IR analysis indicated characteristic bending vibrations of Al-OH bands at 698 cm⁻¹ and stretching modes at 780, 1056, and 3655 cm⁻¹ for (Si-O and Al-Mg-OH) bands, respectively. SEM micrographs showed surfaces with varying platy polycrystalline particle sizes, while XRF results identified the clay as kaolinite with silicate and alumina > 30 and 16%, respectively. The flooding experiment revealed that the SDS-mediated KB clay NPs (8.33 mM SDS) gave the highest total oil recovery of 66.25 % at 0.10 wt. %. Optimizing oil recovery at 8.33 mM by varying concentrations of KBC2 at 0.05, 0.10, 0.15, 0.20, and 0.25 wt. % gave a remarkable oil recovery rate of 85.27% at 0.15 wt.%. Thus, 0.15 wt. % KBC2 is recommended for application in oil recovery.</p>

Introduction

Crude oil can be recovered from trapped/depleting oil reserves, especially in this era of high population and increased energy demand. Oil can be recovered using conventional methods (primary and secondary) by employing natural reservoir pressure flow/assisted lift such as gas cap drive, gravity drainage, solution drive, water drive, and maintaining the reservoir pressure as a result of pressure drop via gas and water injection [1, 2]. These methods still leave a high percentage of oil trapped in the oil reserves, possibly due to high energy at the water-oil interface and heterogeneity of the reservoir.

Several tertiary recovery methods, known as EOR, have been employed to displace more oil and improve recovery efficiency [3, 4]. Some of the tertiary methods utilize chemicals, heat,

*Corresponding Author: J.L. Konne (E-mail address: konne.joshua@ust.edu.ng)



gas, or microbes to enhance the displacement of oil [5-8]. Research has shown that Chemical Enhanced Oil Recovery (CEOR) using surfactants such as Cetyltrimethylammonium bromide (CTAB), a cationic surfactant [9], Triton X-100 (TX-100), a nonionic surfactant [10], Pickering emulsions involving nonionic surfactants (cetyl polyoxyethylene ether-C16E20) [11] and an anionic surfactant, Sodium dodecyl sulfate (SDS) with silica nanoparticles [12] have been successful and are effective in oil displacement. Some mechanisms employed are reducing the capillary force and thus the interfacial reduction, lowering the viscosity of oil, and modifying the formation's wettability towards a more water-wet condition [13-15].

Clays are minerals majorly comprising hydrated aluminum and/or magnesium phyllosilicates [16]. Clays can be modified to enhance their properties, which can benefit many applications, such as the textile industry, catalysts, medicine, pharmacy, cosmetics, food packaging, and the oil industry [17-23]. Cheraghian *et al.* [22] reported that flooding with clay (local sodium bentonite) NPs and SDS solution improved oil recovery. All oil increments of up to 52% were obtained when nano clay particles with an SDS solution of 1800 ppm were utilized in flooding [22]. Employing cheaper local materials, such as clay, with properties similar to those of some NPs, such as silica NPs, has made using clay an economically viable option, among others.

Gbarakoro *et al.* [18] reported that KB clay possessed a kaolinite clay structure with an aluminum-to-silica ratio of 1:4. Furthermore, Udeh *et al.* [24] successfully studied the interactions and stability of foam generated from SDS-mediated KB clay NPs and reported that SDS-mediated KB clay NPs via the sol-gel route significantly led to particle size variation of the modified clay NPs. These variations created porous spaces in the modified clay matrices, and the batch with the smallest particle size achieved the most stable foam. However, no work has been done on its application in EOR. This work investigates the application of SDS-mediated KB clay NPs at varying SDS concentrations using the sol-gel route and the extent of recovery via a micromodel for the first time.

Materials and Methods

Materials

KB clay particles were collected from Kono-Boue in Khana Local Government Area, Rivers State, Nigeria. Other materials used were crude oil obtained from Obelle well 5, Obelle flow station, Port Harcourt, Rivers State, with 31.14 °API at 29 °C. Oil viscosity and density were 10.4832 cP and 0.8704 g/ml, respectively. Sandstone core samples were washed with distilled water and ethanol to remove impurities and water, respectively; they were dried at 90 °C in an oven for 24 hours. The reagents and equipment used in the flooding experiment were:- 99.9% pure Sodium Dodecyl Sulphate (SDS) (C₁₂H₂₄SO₄Na, M.W. = 288.38 g/mol) purchased from British drug House, UK, sodium chloride salt, distilled water, micro model, weighing balance, magnetic stirrer/bar, oven, and muffle furnace.

Table 1. Properties of core samples

Length (cm)	0.38
Diameter (cm)	0.24
Bulk volume (cm ³)	300
Mass of dry sample (kg)	1.250
Mass of saturated sample (kg)	1.580
Mass of water (g)	330
Porosity (%)	35.00
Pore Volume (cm ³)	105

Methods

Synthesis of Clay NPs

Clay particles were dried in an oven at 120 °C for 3 hours for all moisture to completely evaporate. They were further ground and sieved with a mesh sieve of size 1.00 mm. 15 g of fine clay grains were dissolved in 450 ml of distilled water and stirred magnetically for 90 minutes. The mixture's water was decanted and washed three times, oven-dried for 1 day at 110 °C. The dried particles were calcined in a muffle furnace at 900 °C for 120 minutes.

Synthesis of SDS-Mediated Clay NPs

Varying SDS concentrations of 2, 8, and 14 mM were prepared by dispersing 0.15 g, 0.60 g, and 1.05 g in 200 ml of distilled water and made up to the 250 ml mark. The same procedure was used to prepare SDS-mediated clay NPs, but different concentrations of SDS solutions of 2, 8, and 14 mM were used in place of distilled water.

Clay Nanofluid Preparation

The clay nanofluids were prepared by dispersing 0.1 wt. % of various synthesized clay NPs in a 100 ml volume of distilled water.

Characterization

The analysis of synthesized samples was done using Fourier Transform Infra-red (FT-IR) (Agilent Technology Cary 630 FTIR), X-Supreme 8000 X-ray Fluorescence (XRF), Scanning Electron Microscope (SEM) and X-ray Diffraction (XRD) EMPYREAN diffractometer, with a Cu K α radiation of $\lambda=0.15406$ nm and Cu anode current and voltage of 40 mA and 45kV respectively to determine functional groups, the elemental composition, surface morphologies of the samples and the crystal structures, respectively. FTIR samples were prepared by mixing a small spatula with KBr and pelletizing the mixture with an IR press before analysis. XRF and XRD samples were ground using a mortar and pestle before being placed on a sample holder for analysis. In the case of XRF, 2 g of the ground sample was vacuum-dried for 10 minutes and allowed to run for 10 minutes in the XRF spectrometer, while the XRD sample was run without further pretreatment. SEM samples were used without grinding. Small particles of each were placed on a sticky pad on top of an aluminum stub screwed in a sample holder and slotted into the SEM for analysis.

Flooding Experiments

Experiments were done with core samples in a micro model. The primary and secondary flooding experiments were conducted by flooding the oil-wet core samples with 3% wt. Brine solution. This was after the core samples were first saturated with a brine solution to ensure initial water saturation and injection of three pore volumes of crude oil, left for 2 days to



establish an oil-wet condition. Three pore volumes of each of the prepared clay nanofluids for control and SDS-treated were used in flooding to determine the rate of oil displacement. Each flooding experiment was completed by injecting two pore volumes of brine. This was done for the four different SDS concentrations at 0, 2, 8, and 14 mM, and the values of oil recovered after each experiment were recorded. The flooding experiments were performed at a pressure of 5 psi at 29 °C. The mean values of oil and water recovered were recorded.

The oil saturations (residual and critical), total oil recoveries, and displacement efficiencies were calculated using the Eqs. 1-3, respectively.

$$\text{Residual Oil Saturation} = \frac{\text{Original Oil in place}}{\text{Pore Volume}} \times 100 \quad (1)$$

$$\text{Critical Oil Saturation} = \frac{\text{Volume of oil left after water injection}}{\text{Pore Volume}} \times 100 \quad (2)$$

$$\text{Displacement Efficiency} = 1 - \frac{\text{Original Oil in place}}{\text{Pore Volume}} \times 100 \quad (3)$$

Result and Discussion

Characterization

FT-IR

The FT-IR spectra of the control experiment (KBC0) and SDS-mediated clay NPs (KBC1, KBC2, and KBC3) were analyzed within 4000 – 650 cm⁻¹ band ranges. The absorption bands shown in Fig. 1 and Table 2 consist of absorption peaks for Si-O vibrational stretching at 1052 - 1056 cm⁻¹ and 780 cm⁻¹, which correspond to bands associated with the presence of silicate layers such as kaolinite [25-29]. The band at 698 cm⁻¹ was assigned to Al-OH bending, while absorption peaks at 3655 and 3555 cm⁻¹ correspond to Al/Mg-O-H Stretching vibrations [25, 28].

Table 2. FT-IR of KBC0, KBC1, KBC2, and KBC3

KB Clay NPs Ctrl (KBC0)	KB Clay NPs 2 mM (KBC1)	KB Clay NPs 8 mM (KBC2)	KB Clay NPs 14 mM (KBC3)	Assigned Absorption Band
3655	3555	-	3655	Al/Mg-O-H Stretching
1056	1056	1056	1052	Si-O Stretching
780	780	780	780	Si-O Stretching
698	695	698	698	Al-OH Bending

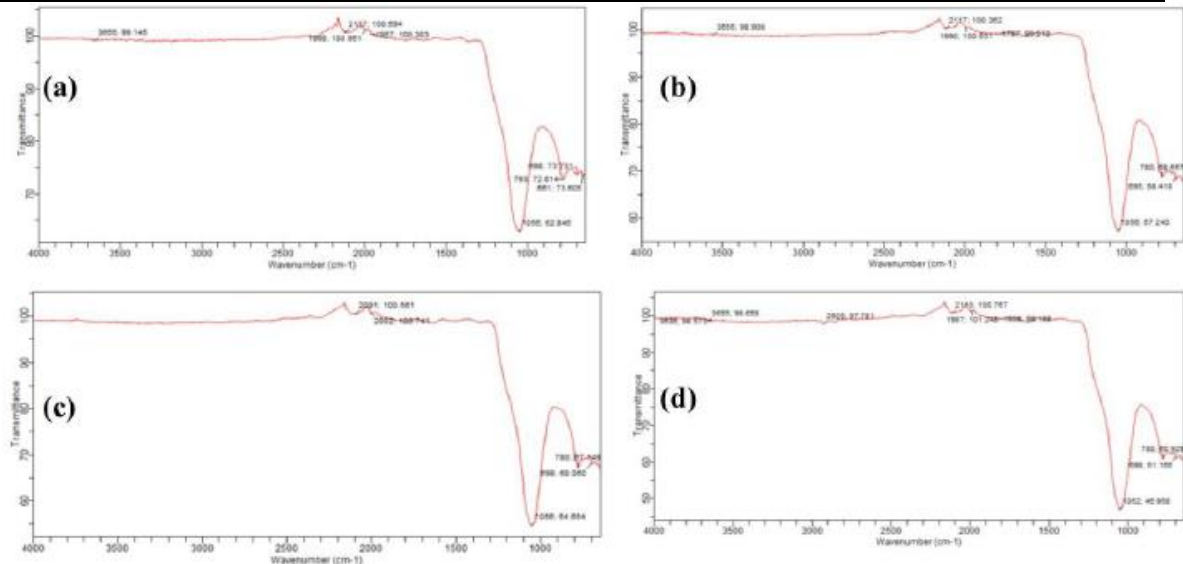


Fig.1. FT-IR spectra for (a) KBC0, (b) KBC1, (c) KBC2 and (d) KBC3

SEM

The SEM micrographs for the clay NPs (control experiment) and SDS-mediated clay NPs (Fig. 2) were taken at 1000 magnification (1000X) with a scale bar of 268 μm (for ease of comparison). The surface morphologies show that the samples form polycrystalline aggregates in platy forms. More porous aggregates were observed in SDS-mediated clay NPs (KBC1, KBC2, and KBC3) than in the control (KBC0). The smallest-sized particles were observed in KBC2, which was prepared with the SDS solution at CMC (8.33 mM) [29].

XRD

The XRD diffraction patterns for KBC0, KBC1, KBC2, and KBC3 are shown in Fig. 3. The presence of two major peaks at 2θ , 21° and 27° agreed with the kaolinite structure of KB clay reported by Gbarakoro *et al.* [18]. The average particle size estimated from Scherrer's formula using the XRD data also confirmed that particles of KBC2 had the smallest particle size [24].

XRF

The elemental compositions of the samples are shown in Table 3, with major elements such as Si and Al having approximately 30% and greater than 16%, respectively, confirming the KB clay NPs as kaolinites. Minor elements like Mg, Fe, and a few trace elements of S, Ti, and K were also observed [18].

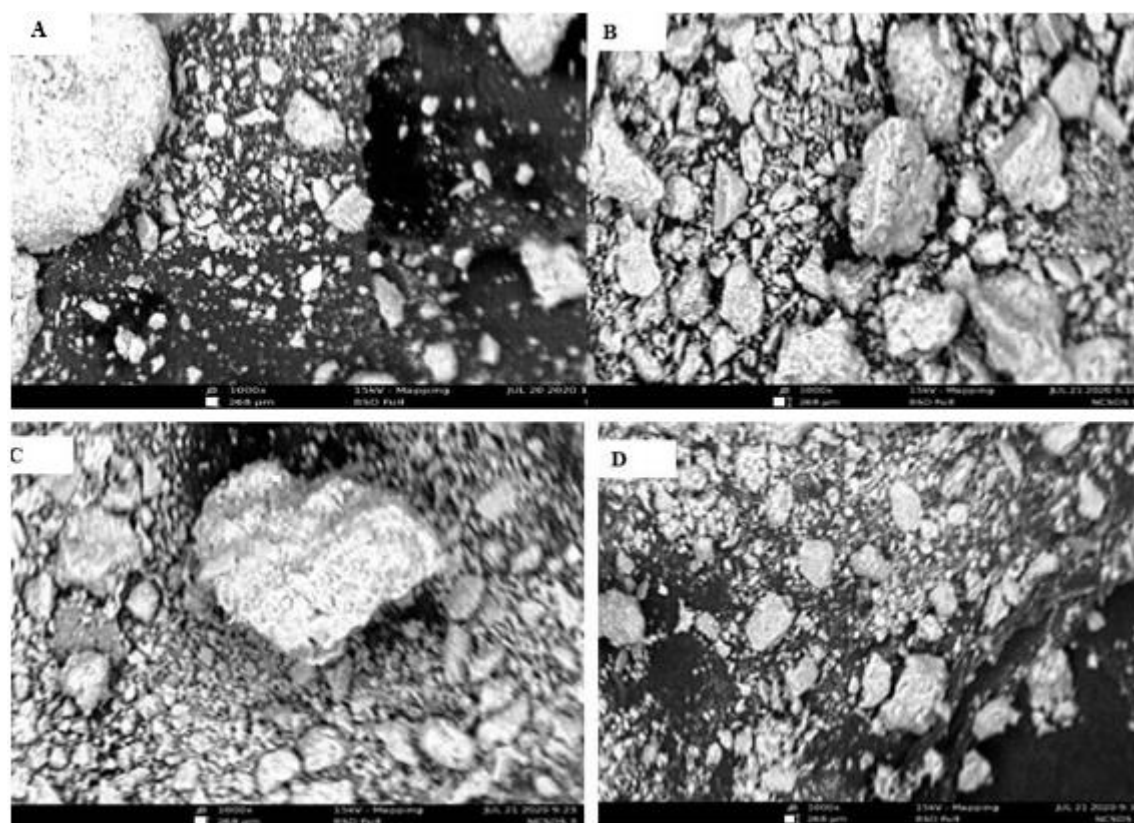


Fig. 2. Surface morphologies of (a) KB Clay NPs Control, (b) KB Clay NPs 2mM, (c) KB Clay NPs 8mM, and (d) KB Clay NPs 14mM

Table 3. Percentage Elemental Composition of KBC0, KBC1 and KBC3

Elements (%)	KBC0	KBC1	KBC3
Si	30.10	29.83	29.38
Al	16.96	16.19	16.15
Fe	2.34	2.20	2.18
Mg	2.09	1.76	2.34
S	0.04	0.20	0.29
Ti	0.81	0.77	0.78
K	0.95	0.93	0.93
Si/Al	1.78	1.84	1.82

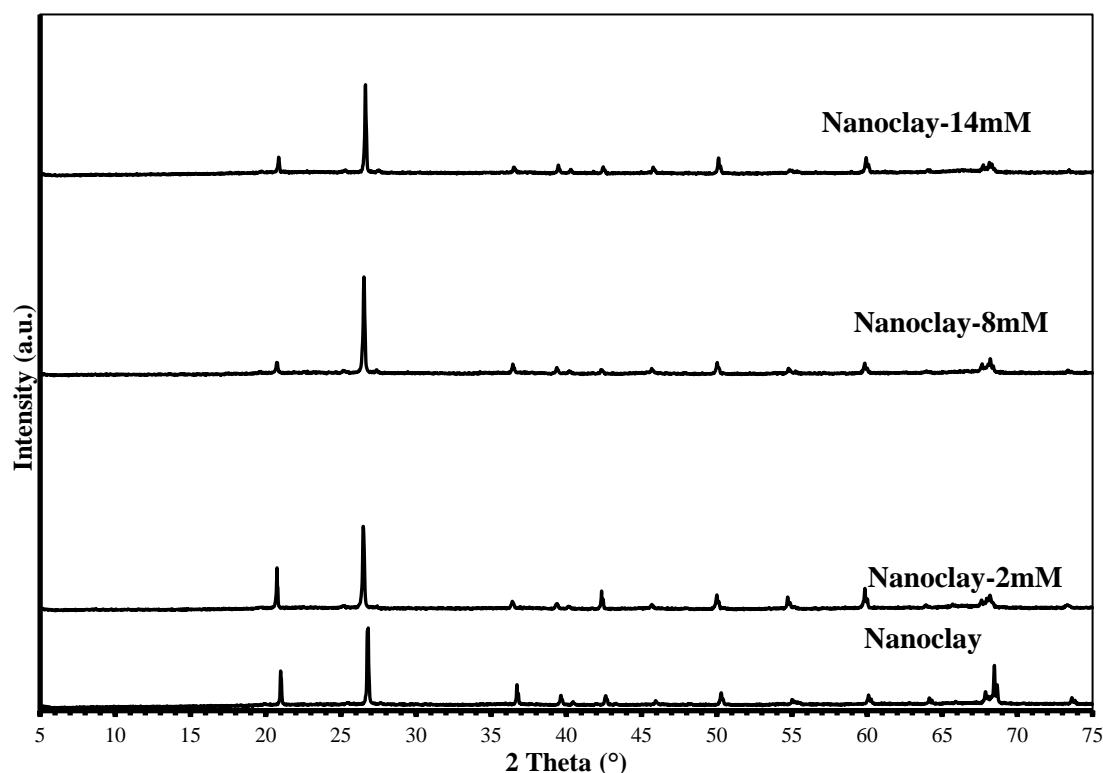


Fig. 3. XRD of KBC0, KBC1, KBC2 and KBC3

Micromodel Results

Oil saturations, as well as total oil recoveries, are terms used to discuss the displacement of oil from core samples in the model. Flooding the model with equal pore volumes of brine solution gave residual oil saturations, as presented in Table 4, denoting the oil percentage left after primary and secondary flooding. Close results of residual oil saturations for both the mediated (control and SDS-treated) clay NPs suggest similar flooding properties and represent the conventional method of oil recoveries [30]. However, flooding the model with the four prepared clay nanofluids (KBC0, KBC1, KBC2, and KBC3) showed a decrease/reduction in oil saturation from higher residual saturation to relatively lower critical oil saturation values. [31] This suggests that the synthesized KB clay NPs interacted with oil/rock and favorably modified the properties of the oil (Fig. 4).

It could be attributed to the recovery mechanisms, which include lowering the capillary force between water and oil, reducing interfacial tension, and altering rock wettability from oil-wet towards water-wet conditions [31-32]. The displacement of oil from trapped oil pockets is also achieved as oil viscosity reduces [15, 32, 33]. The displacement of oil was mostly achieved in KBC2, as clearly shown in EOR efficiency of 21.91% as against those obtained with KBC0, KBC1, and KBC3, which were 8.58%, 19.39%, and 12.77%, respectively (Figs 4 & 5). The EOR efficiency of KBC2 was also greater than the 20% reported in recent literature [12]. This could result from more particle aggregation on the surface of KBC2 (Fig. 2c), probably due to the exit of SDS, which left numerous porous spaces on the surface during calcination and subsequently resulted in particle size variation.

The result aligns with the report analyzed by Udeh *et al.* [24]. Small particles could penetrate more into tiny, porous spaces, displacing the oil passed by water, yielding a total oil recovery of 66.25%. Additionally, KBC2 had the SDS concentration at the CMC, which agrees with the report by Cheraghian and Seyyed [22]. The optimum total oil recovery of KBC2 was determined by varying its concentrations as 0.05, 0.10, 0.15, 0.20, and 0.25 wt. %. This optimization process gave the highest recovery of 85.27% at 0.15 wt. % and at constant SDS concentrations of 8 mM (Fig. 6). This could be attributed to an increase in concentration of

KBC2, which made the interface adsorb more NPs and exert pressure on the oil droplets. Such a process could lower the IFT and significantly alter the wettability from more oil-wet to more water-wet conditions, enhancing the recovery process's efficiency. However, a decrease in efficiency was observed after 0.15 wt. % could be linked to log jamming of NPs accumulation, causing pore throat blockage [32].

Oil Saturations

Table 4. Fluid saturations of KB Clay/SDS nanofluids

KB Clay/SDS nanofluids	Residual oil saturation (%)	Critical oil saturation (%)
KBC0	58.48	49.90
KBC1	56.22	36.83
KBC2	55.66	33.75
KBC3	57.92	45.15

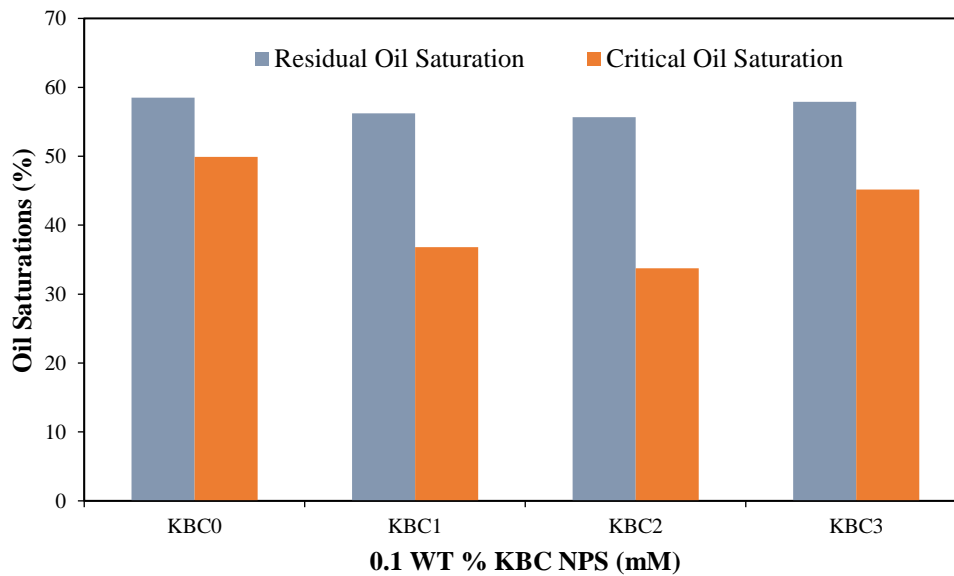


Fig. 4. Oil Saturations of 0.1 wt. % KB Clay NPs

Table 5. Oil Recoveries of KB Clay SDS Mediated NPs

SDS-mediated clay NPs	1° (before application) (%)	3° (EOR) (after application) (%)	Total Oil Recovery (%)	Displacement Efficiency (%)
KBC0	41.52	8.58	50.1	14.67
KBC1	43.78	19.39	63.17	34.49
KBC2	49.34	21.91	66.25	39.36
KBC3	42.08	12.77	54.85	22.05

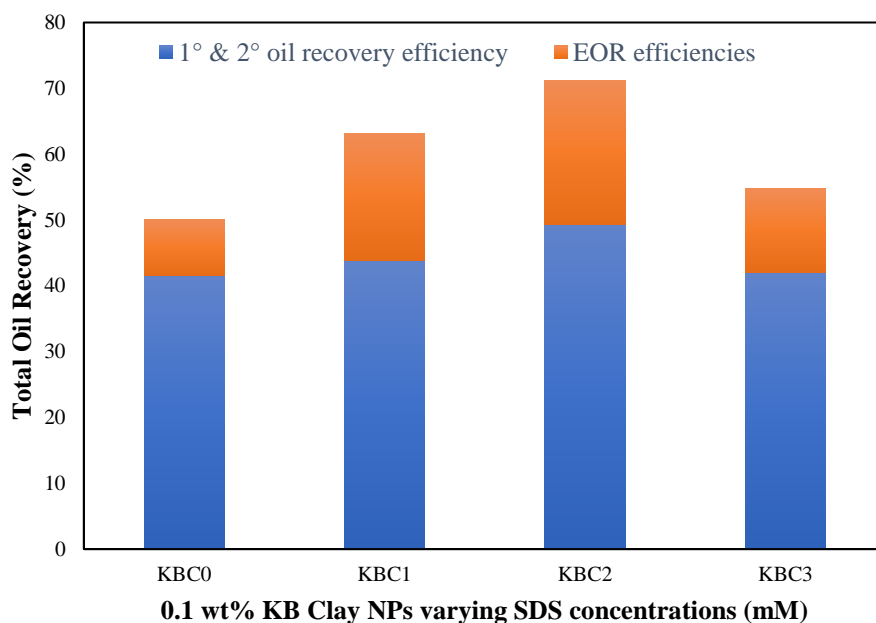


Fig. 5. Total Oil Recoveries of 0.1 wt. % KB Clay NPs

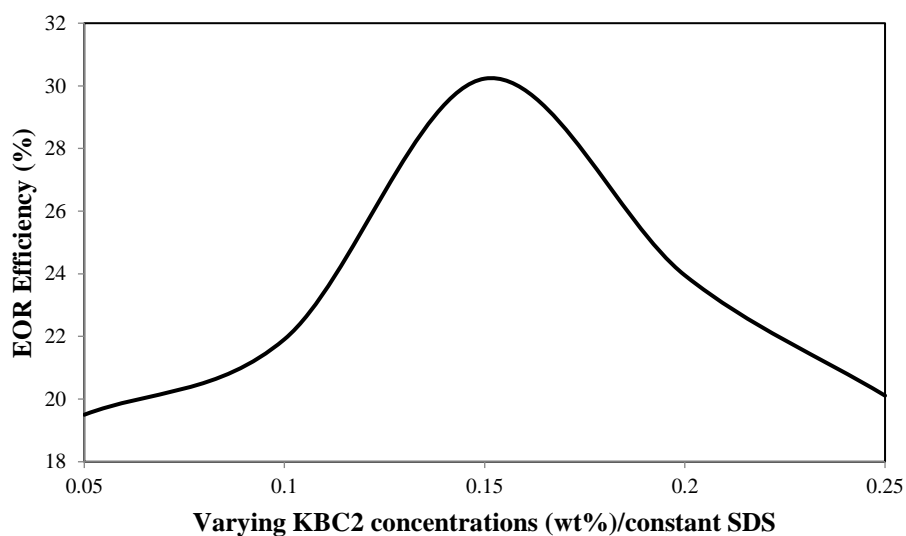


Fig. 6. EOR Efficiency for Optimized KBC2 Concentrations

Conclusion

SDS-mediated KB clay NPs have been synthesized and characterized, and the resultant nanofluids have been employed in flooding in an oil recovery experiment for the first time. The XRD pattern confirmed the KB clay as having a kaolinite structure, while the FT-IR analysis obtained showed stretching and bending vibrations of Si-O and Al-OH at 780, 1056, and 698 cm^{-1} , respectively. SEM results showed polycrystallites in platy forms, while the XRF results confirmed the silica and alumina as having the highest percentages of Si > 30 and Al > 16%, respectively. Experiments on core flooding showed a total oil recovery of 66.25 % with an EOR efficiency of 21.91 % obtained by flooding 0.1 wt. % of KBC2 with 8.33 wt. % SDS and applying the optimized approach by varying KBC2 concentrations gave a record high recovery efficiency of 85.27% at 0.15 wt.%.

Acknowledgment

The authors of this work sincerely thank the Tertiary Educational Trust Fund (TETFUND) for the financial support provided during this research through the Institution Based Research (IBR) Grant of Rivers State University, Port Harcourt, Nigeria, and the Umaru Musa Yar'adua University Central Research Laboratory for the XRD, SEM, FT-IR and XRF analyses.

References

- [1] Omar C. Innovation in Enhanced Oil Recovery. *Recent Advances in Petrochemical Science*. 2018; 5(2). DOI: [10.19080/RAPSCI.2018.05.555659](https://doi.org/10.19080/RAPSCI.2018.05.555659).
- [2] Massarweh O, Abushaikha, AS. The use of surfactants in enhanced oil recovery: A review of recent advances. *Energy Reports*. 2020;6:3150–3178. <https://doi.org/10.1016/j.egy.2020.11.009>.
- [3] Li K, Wang D, Jiang S. Review on enhanced oil recovery by nanofluids. *Oil & Gas Science and Technology – Revue d' IFP Energies nouvelles*. 2018;73(37) <https://doi.org/10.1051/ogst/2018052>.
- [4] Brantson ET, Ju B, Appau PO, Akwensi PH, Peprah GA, Liu N, Aphu ES, Boah EA, Borsah AA. Development of hybrid low salinity water polymer flooding numerical reservoir simulator and smart proxy model for chemically enhanced oil recovery (CEOR). *Journal of Petroleum Science and Engineering*. 2020;187,106751. <http://dx.doi.org/10.1016/j.petrol.2019.106751>.
- [5] Pothula GK, Vij RK, Bera A. An overview of chemically enhanced oil recovery and its status in India. *Petroleum Science*. 2023;20(4): 2305-23.
- [6] Mokheimer EMA, Hamdy M, Abubakar Z, Shakeel MR, Habib MA, Mahmoud M. A comprehensive review of thermally enhanced oil recovery: Techniques evaluation. *Journal of Energy Resources Technology*. 2019;141(3):030801. <http://dx.doi.org/10.1115/1.4041096>.
- [7] Song ZJ, Li M, Zhao C, Yang YL, Hou JR. Gas injection for enhanced oil recovery in a two-dimensional geology-based physical model of Tahe fractured-vuggy carbonate reservoirs: karst fault system. *Petroleum Science*. 2020;17:19-33.
- [8] Niu J, Liu Q, Lv J, Peng B. Review on microbial enhanced oil recovery: Mechanisms, modeling and field trials. *Journal of Petroleum Science and Engineering*. 2020;192,107350. <http://dx.doi.org/10.1016/j.petrol.2020.107350>.
- [9] Shahbazi S, Goodpaster JV, Smith GD, Becker T, Lewis SW. Preparation, characterization and application of a lipophilic coated exfoliated Egyptian blue for near- infrared luminescent latent fingerprint detection. *Forensic Chemistry*, 2020;18,100208. <http://dx.doi.org/10.1016/j.forc.2019.100209>.
- [10] Hosseini S, Experimental investigation of effect of asphaltene deposition on oil relative permeability, rock wettability alteration and oil recovery in WAG process. *Petroleum Science and Technology*. 2019;37(20):2150-2159. <http://dx.doi.org/10.1080/10916466.2018.1482335>.
- [11] Yang L, Ge J, Wu H, Li X, Li J, Zhang G. Study on the Enhanced Oil Recovery Properties of the Pickering Emulsions for Harsh Reservoirs. *ACS Omega*. 2024; DOI: [10.1021/acsomega.4c06834](https://doi.org/10.1021/acsomega.4c06834).
- [12] Wu Y, Chen W, Dai C, Huang Y, Li H, Zhao M, He L, Jiao B. Reducing surfactant adsorption on rock by silica nanoparticles for enhanced oil recovery. *Petroleum of Science and Engineering*. 2017;153, 283-287. <http://dx.doi.org/10.1016/j.petrol.2017.04.015>.
- [13] El-hoshoudy AN, Desouky SEM, Elkady MY, Al-Sabagh AM, Betiha MA, Mahmoud S. Hydrophobically associated polymers for wettability alteration and enhanced oil recovery – Article review. *Egyptian Journal of Petroleum*. 2017; 26(3): 757–762. <http://dx.doi.org/10.1016/j.ejpe.2016.10.008>.

- [14] Zhu D, Hou J, Wang J, Wu X, Wang P, Bai B. Acid-alternating base (AAB) technology for blockage removal and enhanced oil recovery in sandstone reservoirs. *Fuel*. 2018; 215: 619–630. <http://dx.doi.org/10.1016/j.fuel.2017.11.090>.
- [15] Almubarak M, Alyousef Z, Almajid M, Almubarak T, Ng JH. Enhancing foam stability through a combination of surfactant and nanoparticles. In: Abu Dhabi International Petroleum Exhibition and Conference. 2020; <https://doi.org/10.2118/202790-MS.OnePetro>.
- [16] Gamoudi S, Srasra E. Modification of Clay Minerals by Surfactant Agents: Structure, Properties and New Applications. In: *Surfactants-Fundamental Concepts and Emerging Perspectives*. 2024, doi: [10.5772/intechopen.110317](https://doi.org/10.5772/intechopen.110317).
- [17] Choi YS, Cho JH. Color removal dyes from wastewater using vermiculite. *Environmental Technology*. 1996;17:1169-1180.
- [18] Gbarakoro SL, Konne JL, Boisa N. Characterization of Kono-Boue clay as possible catalyst for biodiesel production. *International Journal of Science and Research (IJSR)*, 2016;5(6):924-928. <http://dx.doi.org/10.21275/v5i6.NOV164059>.
- [19] Selvasdha N, Dhanalekshmi UM, Krishnaraj S, Harish Sundar Y, Sri Durga Devi N, Sarathchandiran I. Multifunctional Clay in Pharmaceuticals. In: *Clay Science and Technology*. 2021; <http://dx.doi.org/10.5772/intechopen.92408>.
- [20] Moraes JD, Bertilino R, Cuffini SL, Ducart DF, Bretzke PE, Leonardi GR. Clay minerals: Properties and applications to dermocosmetic products and perspectives of natural raw materials for therapeutic purposes- A review. *International journal of pharmaceutics*. 2017; 534(1-2):213-9.
- [21] Gbarakoro SL, Konne JL, Ofodile S. Synthesis and Evaluation of Biodiesel Using Calcined and Acid Modified Kono-Boue Clays as Catalyst, *International Journal of Chemistry and Chemical Processes*. 2018; 4(1): 2545 – 5265.
- [22] Cheraghian G, Seyyed SK. Improvement of heavy oil recovery and role of nanoparticles of clay in the surfactant flooding process, *Petroleum Science and Technology*, 2016; 34(15): 1397-1405, DOI: [10.1080/10916466.2016.1198805](https://doi.org/10.1080/10916466.2016.1198805).
- [23] Naman K, Sudhanshu S. Exfoliation and Extraction of Nanoclay from Montmorillonite Mineral Rich Bentonite Soil, *IACMAG_Symposium*. 2020;56. https://doi.org/10.1007/978-981-15-0890-5_1.
- [24] Udeh OV, Konne JL, Cookey GA, Nmegbu GJC. Foam Stabilization and Interactive Properties of Kono-Boue Clay Nanoparticles in Oil Recovery. *Journal of Chemical Society of Nigeria*. 2022; 47(4). <https://doi.org/10.46602/jcsn.v47i4.799>.
- [25] Nandiyanto ABD, Oktiano R, Ragadhita R. (2019), How to Read and Interpret FTIR, Spectroscopy of Organic material, *Indonesian Journal of Science and Technology*, 2019;4(1): 97-118. doi: [10.17509/ijost.v4i1.15806](https://doi.org/10.17509/ijost.v4i1.15806).
- [26] Hossain T, Alam MA, Rahman MA, Sharafat MK, Minami H, Gafur MA, Ahmad H, Zwitterionic poly (2-(methacryloyloxy) ethyl phosphrylcholine) coated mesoporous silica particles and doping with magnetic nanoparticles. *Colloids and Surfaces. A: Physicochemical and Engineering Aspects*. 2018;555:80-87. <https://doi.org/10.1016/j.colsurfa.2018.06.020>.
- [27] Sarker MZ, Rahman MM, Minami H, Suzuki T, Ahmad H. Amine functional silica-supported bimetallic Cu-Ni nanocatalyst and investigation of some typical reductions of aromatic nitro substituents. *Colloid and Polymer Science*. 2022; 1:1-8.
- [28] Nayak PS, Singh BK. Instrumental characterization of clay by XRF, XRD and FTIR, *Bulletin of Materials Science*. 2007;30(3). 235-238. <http://dx.doi.org/10.1007/s12034-007-0042-5>.
- [29] Sadri N, Baghernejad M, Ghasemi-Fasaei R, Moosavi AA, Hardie AG. Characterization of clay and nanoclay extracted from a semi-arid Vertisol and Investigation of their carbon sequestration potential. *Environmental Monitoring and Assessment*. 2024;196(1):96. doi: [10.1007/s10661-023-12246-x](https://doi.org/10.1007/s10661-023-12246-x). PMID: 38153593.
- [30] Onyekonwu MO, Ogolo NA. Investigating the use of nanoparticles in enhancing oil recovery. In: *SPE Nigeria Annual International Conference and Exhibition 2010*; SPE-140744.



- [31] Rezvani H, Binks BP, Ngugen D, Surfactant-Nanoparticles Formulations for Enhanced Oil Recovery in Calcite-Rich Rocks. *Langmuir: the ACS journal of surfaces ad colloids*, 2024; 40(47):24989-25002. <https://doi.org/10.1021/acs.langmuir.4c03100>.
- [32] Konne JL, Udeh OV, Cookey, GA, & Nmegbu GCJ. Surfactant (Sodium Dodecyl Sulphate) Coated Silica (SiO₂) Nanoparticles for Enhanced Oil Recovery: An Optimized Approach. *Iranian Journal of Oil and Gas Science and Technology*. 2022; 11(2): 65- 80. doi: [10.22050/ijogst.2022.334848.1632](https://doi.org/10.22050/ijogst.2022.334848.1632).
- [33] Al-Anssari S, Arif M, Wang S, Barifcani A, Iglauer S Stabilizing nanofluids in saline environments. *Journal of Colloid Interface Science*. 2017; 508, 222–229. <https://doi.org/10.1016/j.jcis.2017.08.043>.

How to cite: Udeh O.V, Konne J.L, Cookey G.A, Nmegbu G.C.J. Application of Surfactant Modified Kono-Boue Clay Nanoparticles in Oil Recovery. *Journal of Chemical and Petroleum Engineering* 2025; 59(1): 173-184.